Available at
http://pvamu.edu/aam
Appl. Appl. Math.
ISSN: 1932-9466

Applications and Applied Mathematics:
An International Journal
(AAM)

Vol. 11, Issue 2 (December 2016), pp. 693 - 703

Unsteady MHD Flow Past an Impulsively Started Inclined Plate with Variable Temperature and Mass Diffusion in the presence of Hall current

U. S. Rajput and Gaurav Kumar
Department of Mathematics and Astronomy
University of Lucknow
U.P, India
Email: rajputgauravlko@gmail.com

Received: December 10, 2015; Accepted: July 21, 2016

Abstract

In the present paper, we study the effect of Hall current on unsteady flow of a viscous, incompressible and electrically conducting fluid past an impulsively started inclined plate with variable temperature and mass diffusion in the presence of transversely applied uniform magnetic field. The plate temperature and the concentration level near the plate increase linearly with time. The parameters considered in the model are: angle of the plate measured from the vertical, thermal Grashof number, mass Grashof Number, Prandtl number, Hall current parameter, the magnetic field parameter, Schmidt number and time. The fluid model under consideration has been solved by Laplace transform technique. The model contains equations of motion, diffusion equation and equation of energy. To analyze the solution of the model, desirable sets of the values of the parameters have been considered. The numerical data obtained is discussed with the help of graphs and table. The numerical values obtained for skin-friction have been tabulated. We found that the values obtained for velocity, concentration and temperature are in concurrence with the actual flow of the fluid. The motive of this study is to analyze the Hall effect in the model. In the study we found that the velocity in the boundary layer increases with the values of Hall current parameter. It is also observed that the Hall current increases the drag at the plate surface. The importance of the problem can be seen in cooling of electronic components of a nuclear reactor, bed thermal storage and heat sink in the turbine blades.

Keywords: MHD flow; inclined plate; variable temperature; mass diffusion; Hall current

MSC 2010 No.: 76W05, 76D05

1. Introduction

MHD flow problems associated with heat and mass transfer plays an important role in different areas of science and technology. The effect of variable properties on the unsteady Hartmann flow with heat transfer considering the Hall effect was considered by Attia (2003). Further, Attia along with Sayed (2004) has investigated the Hall effect on unsteady MHD Couette flow with heat transfer of a Bingham fluid with suction and injection. In both the models mentioned, the governing non-linear equations of motion have been solved by numerical methods. MHD transient flow past an impulsively started infinite horizontal porous plate in a rotating system with Hall current was studied by Ahmed and Sarmah (2010). It was observed by Ahmed and Sharma (2010) that magnetic field (applied) retards the fluid velocity. Satya et al. (2011) have considered Hall current effect on free convection MHD flow past a porous plate. Further, Jacob et al. (2012) have studied magnetic field and Hall current effects on MHD free convection flow past a vertical rotating plate. Hall effect on transient MHD flow past an impulsively started vertical plate in a porous medium with ramped temperature, rotation and heat absorption was examined by Ahmed and Das (2013). Chemical reaction and Hall effects on MHD convective flow along an infinite vertical porous plate with variable suction and heat absorption was investigated by Masthanrao et al. (2013). Similar studies were done by Jaimala et al. (2013), Naik et al. (2014), Srinivas and Naikoti (2015), and Abdel and Qatanani (2016). Rajput and Kumar (2011) have worked on MHD flow past an impulsively started vertical plate with variable temperature and mass diffusion. They (Rajput and Kumar (2011)) solved the governing flow model by using Laplace transform technique, and observed that the magnetic field parameter slows down the velocity of the flow. We, in a sense, are extending the work of Rajput and Kumar (2011) to study the effect of Hall current in the flow model. The effect of Hall current on the velocity is observed with the help of graphs. The skin friction has been tabulated.

2. Mathematical Analysis

The geometrical model of the problem is shown in Figure 1.

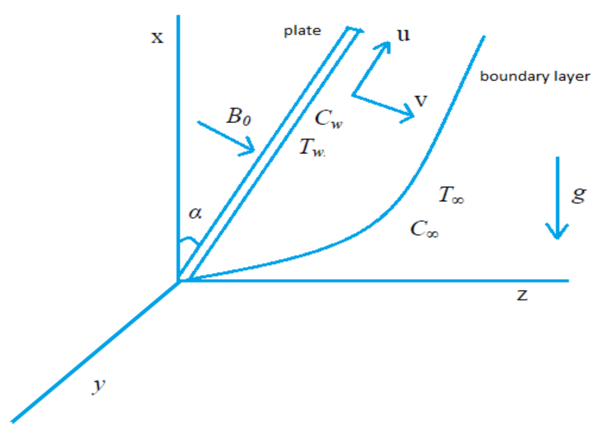

Figure 1. Physical model

The x axis is taken along the vertical plane and z axis is normal to it. Thus, the z axis lies in the horizontal plane. The plate is inclined at angle α from vertical. The magnetic field B_0 of uniform strength is applied perpendicular to the flow. During the motion, the direction of the magnetic field changes along with the plate in such a way that it always remains perpendicular to it. This means, the direction of magnetic field is tied with the plate. Initially it has been considered that the plate as well as the fluid is at the same temperature T_∞. The species concentration in the fluid is taken as C_∞. At time $t > 0$, the plate starts moving with a velocity u_0 in its own plane and temperature of the plate is raised to T_w. The concentration C_w near the plate is raised linearly with respect to time. Due to the Hall effect there will be two components of the momentum equation.

The flow model is as follows.

$$\frac{\partial u}{\partial t}=\upsilon\frac{\partial^2 u}{\partial z^2}+g\beta Cos\alpha\,(T-T_\infty)+g\beta^* Cos\alpha\,(C-C_\infty)-\frac{\sigma B_0^2(u+mv)}{\rho(1+m^2)}, \tag{1}$$

$$\frac{\partial v}{\partial t}=\upsilon\frac{\partial^2 v}{\partial z^2}+\frac{\sigma B_0^2(mu-v)}{\rho(1+m^2)}, \tag{2}$$

$$\frac{\partial C}{\partial t}=D\frac{\partial^2 C}{\partial z^2}, \tag{3}$$

$$\rho C_p\frac{\partial T}{\partial t}=k\frac{\partial^2 T}{\partial z^2}. \tag{4}$$

The initial and boundary conditions are:

$$\left.\begin{array}{l} t\le 0: u=0,\ v=0,\ T=T_\infty,\ C=C_\infty,\ \text{ for all } z,\\ t>0: u=u_0,\ v=0,\ T=T+(T_w-T_\infty)\dfrac{u_0^2 t}{\upsilon},\ C=C_\infty+(C_w-C_\infty)\dfrac{u_0^2 t}{\upsilon},\ \text{ at } z=0,\\ u\to 0,\ v=0,\ T\to T_\infty,\ C\to C_\infty,\ \text{ as } z\to\infty. \end{array}\right\} \tag{5}$$

Here, u and v are the primary and secondary velocities along x and z directions respectively, g-the acceleration due to gravity, β -volumetric coefficient of thermal expansion, t-time, $m(=\omega_e\tau_e)$ -the Hall current parameter with ω_e -cyclotron frequency of electrons and τ_e -electron collision time, T-temperature of the fluid, β^* - volumetric coefficient of concentration expansion, C-species concentration in the fluid, ν- the kinematic viscosity, ρ- the density, C_p- the specific heat at constant pressure, k- thermal conductivity of the fluid, D-the mass diffusion coefficient, K- the permeability parameter, T_w - temperature of the plate at $z= 0$, C_w -species concentration at the plate $z= 0$, B_0- the uniform magnetic field, and σ - electrical conductivity.

The following non-dimensional quantities are introduced to transform Equations (1), (2), (3) and (4) into dimensionless form:

$$\left.\begin{array}{l} \bar{z}=\dfrac{zu_0}{\upsilon},\ \bar{u}=\dfrac{u}{u_0},\ \bar{v}=\dfrac{v}{u_0},\ \theta=\dfrac{(T-T_\infty)}{(T_w-T_\infty)},\ S_c=\dfrac{\upsilon}{D},\ \mu=\rho\upsilon, \bar{C}=\dfrac{(C-C_\infty)}{(C_w-C_\infty)},\\ G_r=\dfrac{g\beta\upsilon(T_w-T_\infty)}{u_0^{3}},\ M=\dfrac{\sigma B_0^2\upsilon}{\rho u_0^2},\ G_m=\dfrac{g\beta^*\upsilon(C_w-C_\infty)}{u_0^{3}},\ P_r=\dfrac{\mu u_0}{k},\ \bar{t}=\dfrac{tu_0^2}{\upsilon}. \end{array}\right\} \tag{6}$$

The symbols in dimensionless form are:

$\bar{u}$ - primary velocity, $\bar{v}$ -secondary velocity, $\bar{t}$ -time, θ- temperature, $\overline{C}$ -concentration, G_r- thermal Grashof number, G_m- mass Grashof number, μ- coefficient of viscosity, P_r -Prandtl number, S_c -Schmidt number, M- magnetic parameter.

The flow model in dimensionless form is:

$$\frac{\partial \bar{u}}{\partial \bar{t}} = \frac{\partial^2 \bar{u}}{\partial \bar{z}^2} + G_r Cos\alpha\, \theta + G_m Cos\alpha\, \overline{C} - \frac{M(\bar{u} + m\bar{v})}{(1+m^2)}, \tag{7}$$

$$\frac{\partial \bar{v}}{\partial \bar{t}} = \frac{\partial^2 \bar{u}}{\partial \bar{z}^2} + \frac{M(m\bar{u} - \bar{v})}{(1+m^2)}, \tag{8}$$

$$\frac{\partial \overline{C}}{\partial \bar{t}} = \frac{1}{S_c}\frac{\partial^2 \overline{C}}{\partial \bar{z}^2}, \tag{9}$$

$$\frac{\partial \theta}{\partial \bar{t}} = \frac{1}{P_r}\frac{\partial^2 \theta}{\partial \bar{z}^2}. \tag{10}$$

The corresponding boundary conditions (5) become:

$$\left.\begin{array}{ll} \bar{t} \le 0 : \bar{u} = 0,\ \bar{v} = 0,\ \theta = 0,\ \overline{C} = 0, & \text{for all } \bar{z}, \\ \bar{t} > 0 : \bar{u} = 1,\ \bar{v} = 0,\ \theta = \bar{t},\ \overline{C} = \bar{t}, & \text{at } \bar{z} = 0, \\ \bar{u} \to 0,\ \bar{v} \to 0,\ \theta \to 0,\ \overline{C} \to 0, & \text{as } \bar{z} \to \infty. \end{array}\right\} \tag{11}$$

Dropping bars in the above equations, we get

$$\frac{\partial u}{\partial t} = \frac{\partial^2 u}{\partial z^2} + G_r Cos\alpha\, \theta + G_m Cos\alpha\, C - \frac{M(u + mv)}{(1+m^2)}, \tag{12}$$

$$\frac{\partial v}{\partial t} = \frac{\partial^2 v}{\partial z^2} + \frac{M(mu - v)}{(1+m^2)}, \tag{13}$$

$$\frac{\partial C}{\partial t} = \frac{1}{S_c}\frac{\partial^2 C}{\partial z^2}, \tag{14}$$

$$\frac{\partial \theta}{\partial t} = \frac{1}{P_r}\frac{\partial^2 \theta}{\partial z^2}. \tag{15}$$

The boundary conditions become

$$\left.\begin{array}{ll} t \le 0 : u = 0, v = 0, \theta = 0, C = 0, & \text{for all } z, \\ t > 0 : u = 1, v = 0,\ \theta = t,\ C = t, & \text{at } z=0, \\ u \to 0,\ v \to 0,\ \theta \to 0,\ C \to 0, & \text{as } z \to \infty. \end{array}\right\} \tag{16}$$

Writing the Equations (12) and (13) in combined form (using $q= u + i\, v$) gives us the following.

$$\frac{\partial q}{\partial t}=\frac{\partial^2 q}{\partial z^2}+G_r Cos\alpha\,\theta+G_m Cos\alpha\, C-qa, \tag{17}$$

$$\frac{\partial C}{\partial t}=\frac{1}{S_c}\frac{\partial^2 C}{\partial z^2}, \tag{18}$$

$$\frac{\partial \theta}{\partial t}=\frac{1}{P_r}\frac{\partial^2 \theta}{\partial z^2}. \tag{19}$$

Finally, the boundary conditions become

$$\left.\begin{array}{ll} t\le 0: q=0, \theta=0, C=0, & \text{for all z,} \\ t>0: q=1, \theta=t, C=t, & \text{at } \ z=0, \\ q\to 0,\ \theta\to 0,\ C\to 0, & \text{as } \ z\to\infty. \end{array}\right\} \tag{20}$$

Here,

$$a=\frac{M(1-im)}{1+m^2}.$$

The dimensionless governing Equations (17) to (19), subject to the boundary conditions (20), are solved by the usual Laplace Transform technique. The solution obtained is

$$C=t\left\{(1+\frac{z^2 S_c}{2t})erfc[\frac{\sqrt{S_c}}{2\sqrt{t}}]-\frac{z\sqrt{S_c}}{\sqrt{\pi\sqrt{t}}}e^{-\frac{z^2}{4t}S_c}\right\},$$

$$\theta=t\left\{(1+\frac{z^2 P_r}{2t})erfc[\frac{\sqrt{P_r}}{2\sqrt{t}}]-\frac{z\sqrt{P_r}}{\sqrt{\pi\sqrt{t}}}e^{-\frac{z^2}{4t}P_r}\right\},$$

$$\begin{aligned} q=&\frac{1}{2}e^{-\sqrt{a}z}A_{15}+\frac{Cos\alpha}{4a^2\sqrt{\pi}}[\sqrt{\pi}G_r\{-A_9 z+\sqrt{a}e^{-\sqrt{a}z}A_2 z+\frac{1}{2A_{13}A_3}+2e^{-\sqrt{a}z}A_1 P_r+2A_{13}A_3 P_r\} \\ &-G_r P_r\{-aA_{10}z+\frac{1}{\sqrt{P_r}}A_{13}\sqrt{\pi}A_4+\frac{2\sqrt{\pi}A_{11}}{\sqrt{P_r}}-\frac{2a\sqrt{\pi}tA_{11}}{\sqrt{P_r}}+\frac{1}{A_{13}\sqrt{\pi}A_8\sqrt{P_r}}-2\sqrt{\pi P_r}A_{11}\} \\ &-\sqrt{\pi}G_m\{A_9 z-\sqrt{a}e^{-\sqrt{a}z}A_2 z-2e^{-\sqrt{a}z}A_1 S_c+2A_{14}A_5 S_c\}+\sqrt{S_c}G_m\{-aA_{16}z+\frac{1}{\sqrt{\pi S_c}A_{14}A_7} \\ &+\frac{2\sqrt{\pi}A_{12}}{\sqrt{S_c}}+\frac{1}{A_{14}\sqrt{\pi S_c}A_6}-2A_{12}\sqrt{\pi S_c}\}]. \end{aligned}$$

The expressions for the symbols involved in the above solutions are given in the appendix.

3. Skin friction

The dimensionless skin friction at the plate is

$$\left(\frac{dq}{dz}\right)_{z=0} = \tau_x + i\tau_y \ .$$

The numerical values of τ_x and τ_y, for different parameters, are given in Table 1.

4. Results and Discussion

The velocity profiles for different parameters like, thermal Grashof number (G_r), mass Grashof number (G_m), magnetic field parameter (M), Hall parameter (m), Prandtl number (P_r) and time(t) are shown in Figures 1.1 to 2.8. In Figures 1.1 and 2.1, it is observed that the primary and secondary velocities of fluid decrease when the plate angle (α) is increased. This is in agreement with the actual flow, since the velocity of the fluid decreases as we increase the inclination of the plate from the vertical. Figures 1.2, 2.2, 1.3 and 2.3 show the buoyancy effect. It is observed that both the primary and the secondary velocities increase on increasing mass Grashof number (G_m) and thermal Grashof number (G_r). This indicates that buoyancy force in the boundary layer region near the plate tends to accelerate primary and secondary velocities. Also, if Hall current parameter m is increased then u increases, while v gets decreased (Figures 1.4 and 2.4). It is observed from Figures 1.5 and 2.5 that the effect of increasing values of the parameter (M) results in decreasing u and increasing v. It is in agreement since the magnetic field establishes a force which acts against the main flow resulting in slowing down the velocity of fluid. Further, it is observed that velocities decrease when Prandtl number is increased (Figures 1.6 and 2.6). When the Schmidt number is increased the velocities get decreased (Figures 1.7 and 2.7). In actual sense, the increase of Sc means decrease of molecular diffusivity (D). This shows that the process of diffusion will decrease. Further, from Figures 1.8 and 2.8 it is observed that the velocities increase with time.

Skin friction is given in Table 1. The value of τ_x increases with the increase in thermal Grashof number, mass Grashof Number, Hall current parameter and time; and it decreases with the angle of inclination of the plate, the magnetic field, the Prandtl number and the Schmidt number. The value of τ_y increases with the increase in thermal Grashof number, mass Grashof Number, the magnetic field and time; and it decreases with the angle of inclination of plate, Hall current parameter, Prandtl number and Schmidt number.

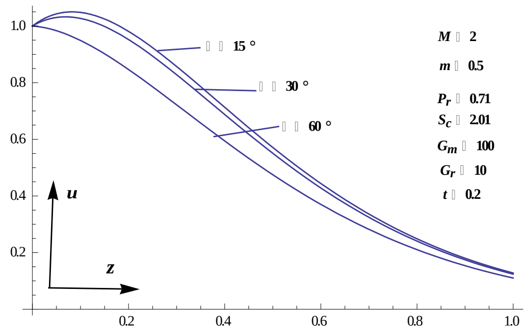

Figure 1.1. Velocity u for different values of α

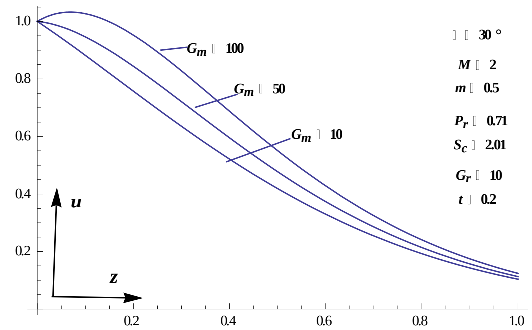

Figure 1.2. Velocity u for different values of *Gm*

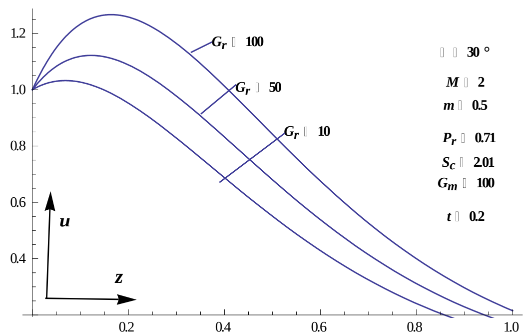

Figure 1.3. Velocity u for different values of *Gr*

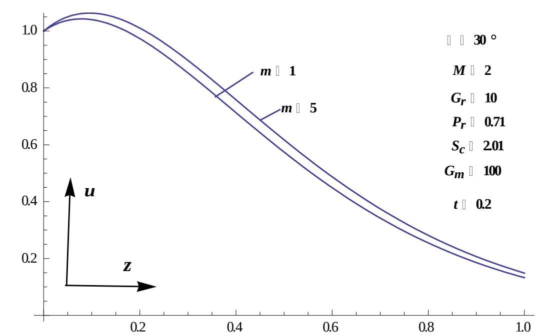

Figure 1.4. Velocity u for different values of *m*

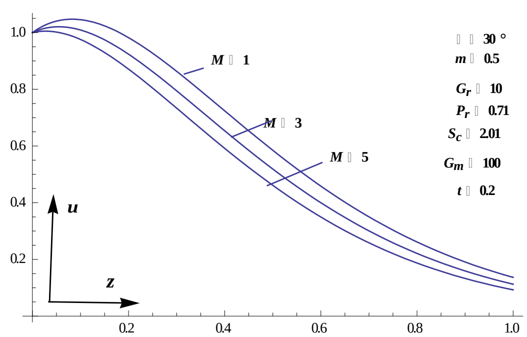

Figure 1.5. Velocity u for different values of *M*

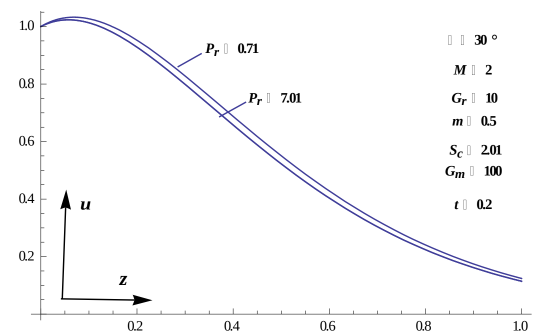

Figure 1.6. Velocity u for different values of *Pr*

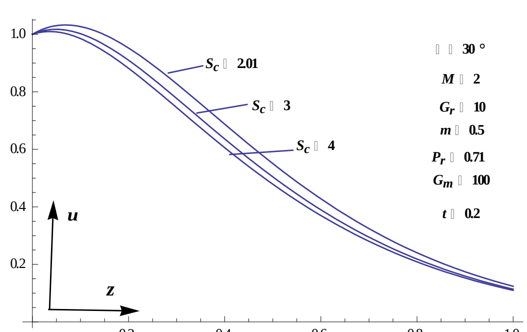

Figure 1.7. Velocity u for different values of *Sc*

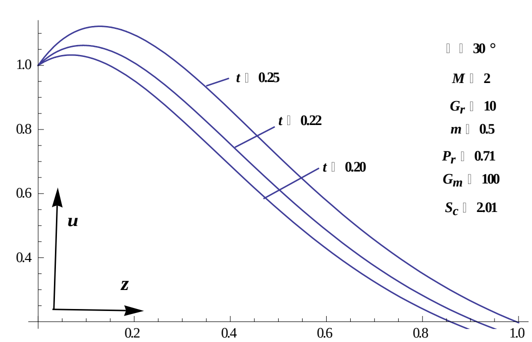

Figure 1.8. Velocity u for different values of *t*

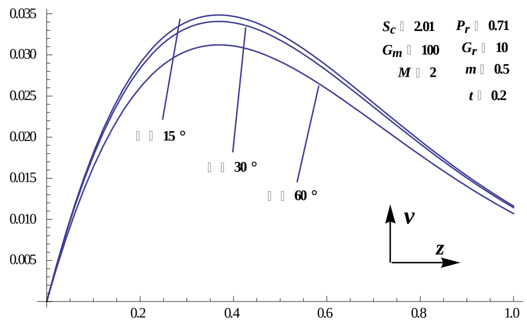

Figure 2.1. Velocity v for different values of *α*

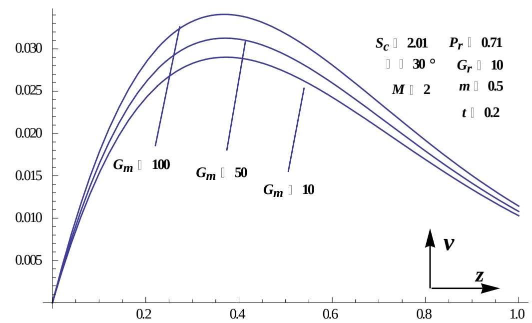

Figure 2.2. Velocity v for different values of *Gm*

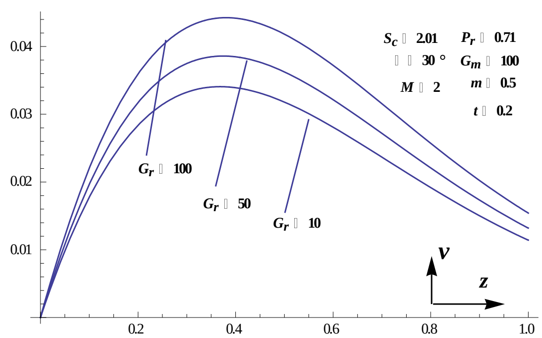

Figure 2.3. Velocity v for different values of *Gr*

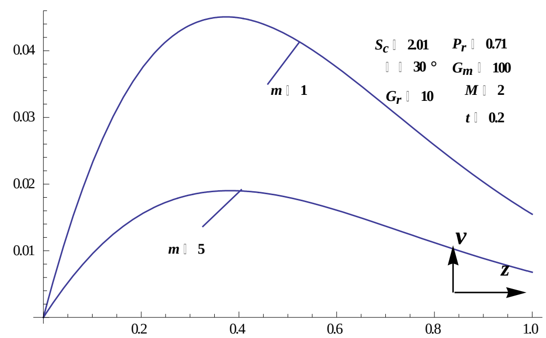

Figure 2.4. Velocity v for different values of *m*

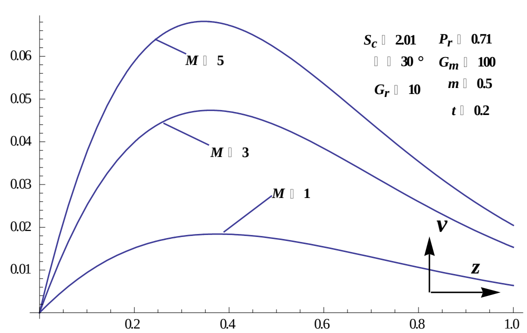

Figure 2.5. Velocity v for different values of *M*

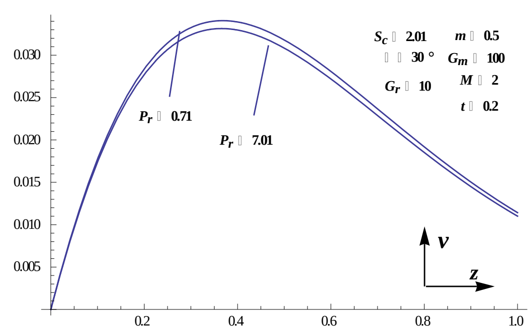

Figure 2.6. Velocity v for different values of *Pr*

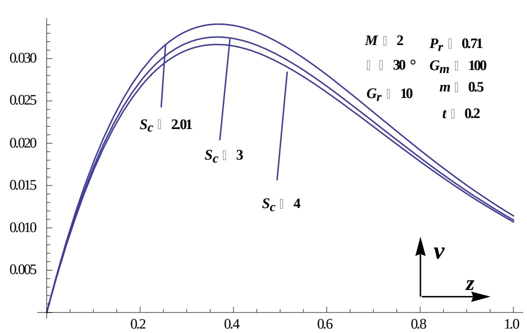

Figure 2.7. Velocity v for different values of *Sc*

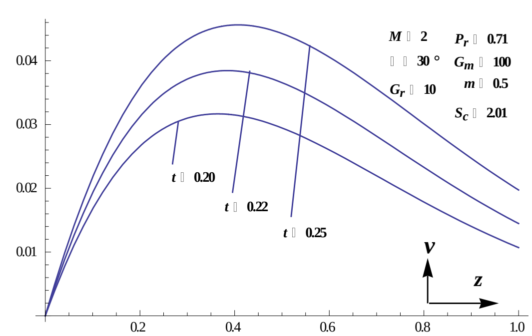

Figure 2.8. Velocity v for different values of *t*

Table 1. Skin friction for different parameters

α *(in degrees)*	M	m	Pr	Sc	Gm	Gr	t	τ_x	τ_y
15	2	0.5	0.71	2.01	100	010	0.20	1.31051	0.220449
30	2	0.5	0.71	2.01	100	010	0.20	1.00438	0.216483
60	2	0.5	0.71	2.01	100	010	0.20	-0.11720	0.201952
30	1	0.5	0.71	2.01	100	010	0.20	1.23007	0.113692
30	3	0.5	0.71	2.01	100	010	0.20	0.78729	0.309671
30	5	0.5	0.71	2.01	100	010	0.20	0.37744	0.471697
30	2	0.5	7.01	2.01	100	010	0.20	0.85575	0.212791
30	2	0.5	13.1	2.01	100	010	0.20	0.82317	0.212303
30	2	1.0	0.71	2.01	100	010	0.20	1.16637	0.280478
30	2	1.5	0.71	2.01	100	010	0.20	1.27661	0.265187
30	2	0.5	0.71	2.01	100	010	0.20	1.00438	0.216483
30	2	0.5	0.71	3.00	100	010	0.20	0.74004	0.210211
30	2	0.5	0.71	4.00	100	010	0.20	0.55817	0.206324
30	2	0.5	0.71	2.01	010	010	0.20	-1.10904	0.190039
30	2	0.5	0.71	2.01	050	010	0.20	-0.16974	0.201792
30	2	0.5	0.71	2.01	100	010	0.20	1.00438	0.216483
30	2	0.5	0.71	2.01	100	010	0.20	1.00438	0.216483
30	2	0.5	0.71	2.01	100	050	0.20	2.22691	0.236482
30	2	0.5	0.71	2.01	100	100	0.20	3.75508	0.261480
30	2	0.5	0.71	2.01	100	010	0.22	1.44557	0.232385
30	2	0.5	0.71	2.01	100	010	0.25	2.12677	0.257492

5. Applications of the study

This study is expected to be useful in understanding the influence of magnetic field and Hall current on astrophysical problems. Moreover, the findings of the research will be useful in improving the devices like Hall accelerators and Hall sensors. It is also useful to study the flow of plasma in MHD power generators, enhanced oil recovery and filtration systems.

6. Conclusion

In this paper a theoretical analysis has been done to study the unsteady MHD flow past an impulsively started inclined plate with variable temperature and mass diffusion in the presence of Hall current. The results obtained are in agreement with the usual flow. It has been found that the velocity in the boundary layer increases with the values of Hall current parameter. It is also observed that the Hall current increases the drag at the plate surface. This work can further be extended by considering some more relevant fluid parameters like chemical reaction, radiation etc. The geometry of the model can also be changed to accommodate some MHD flows with important applications.

REFERENCES

Ahmed, N. and Das, K. Kr. (2013). Hall effect on transient MHD flow past an impulsively started vertical plate in a porous medium with ramped temperature, rotation and heat absorption, Applied Mathematical Sciences, Vol. 7, no. 51, pp. 2525–2535.

Ahmed, N. and Sarmah, H. K. (2010). MHD transient flow past an impulsively started infinite horizontal porous plate in a rotating system with Hall current, Int. J. of Appl. Math and Mech., 7 (2), pp. 1-15.

Attia, H. A. (2003). The effect of variable properties on the unsteady Hartmann flow with heat transfer considering the Hall effect, Appl. Math. Model, 27 (7), pp. 551–563.

Attia, H. A. and Ahmed, M. E. S. (2004). The Hall effect on unsteady MHD Couette flow with heat transfer of a Bingham fluid with suction and injection, Applied Mathematical Modelling, 28, pp.1027-1045.

Jacob, K., Wabomba, M. S., Kinyanjui, A. M. and Lunani, M. A. (2012). Magnetic field and Hall current effect on MHD free convection flow past a vertical rotating flat plate, Asian Journal of Current Engineering and Maths, 6, pp.346-354.

Jaimala, V. and Kumar, V. (2013). Thermal convection in a couple-stress fluid in the presence of horizontal magnetic field with Hall current. Application and applied Mathematics, Vol.8, Issue, pp. 161-117.

Maripala, S. and Naikoti, K. (2015). Hall effect on unsteady MHD free convection flow over a stretching sheet with variable viscosity and viscous dissipation, World Applied Sciences Journal, 33 (6), pp.1032-1041.

Masthanrao, S., Balamurugan, K.S., Varma, S.V.K., and Raju, V. C. C. (2013). Chemical reaction and Hall effects on MHD convective flow along an infinite vertical porous plate with variable suction and heat absorption, Applications and Applied Mathematics, Vol. 8, Issue 1, pp. 268-288.

Naik, H., Murthy, M.V.R., Rao, K. R. (2014). The effect of Hall current on an unsteady MHD free convective Couette flow between two permeable plates in the presence of thermal radiation, International Journal of Computational Engineering Research, Vol 04, Issue 7, pp 40-55.

Rajput, U.S. and Kumar, S. (2011). MHD flow past an impulsively started vertical plate with variable temperature and mass diffusion, Applied Mathematical Sciences, Vol. 5, no. 3, pp.149–157.

Satya, N.P.V., Ramireddy, G. and Venkataramana, S. (2011). Hall current effects on free convection MHD flow past a porous plate, International Journal of Automotive and Mechanical Engineering, Volume 3, pp. 350-363.

Sa’ad Aldin, A. L. and Qatanani, N. (2016). On unsteady MHD flow through porous medium between two parallel flat plates, An - Najah Univ. J. Res.(N. Sc.), Vol. 30(1).

Appendix:

$A_1 = -1 - A_{16} - e^{2\sqrt{az}}(1 - A_{17}),\ A_2 = -1 + A_{16} - e^{2\sqrt{az}}(1 - A_{17}),\ A_8 = -A_4,$

$A_3 = -1 + A_{20} - A_{18}(1 - A_{21}),\ A_4 = 1 + A_{23} + A_{18}(1 - A_{24}),\ A_5 = -1 + A_{25} - A_{19}(1 - A_{26}),$

$A_6 = -1 - A_{27} - A_{19}(1 + A_{28}),\ A_7 = -A_6,\quad A_9 = \dfrac{2e^{-\sqrt{az}}A_1}{z}(1 - at),\quad A_{10} = (2e^{\frac{-z^2 P_r}{4t}}\sqrt{t} + \sqrt{\pi} z A_{11})\sqrt{P_r},$

$A_{11} = -1 + erf[\dfrac{z\sqrt{P_r}}{2\sqrt{t}}],\ A_{12} = -1 + erf[\dfrac{z\sqrt{S_c}}{2\sqrt{t}}],\ A_{13} = e^{\frac{at}{-1+P_r} - z\sqrt{\frac{aP_r}{-1+P_r}}},\ A_{14} = e^{\frac{at}{-1+S_c} - z\sqrt{\frac{aS_c}{-1+S_c}}},$

$A_{15} = 1 + A_{16} + e^{2\sqrt{az}} erfc[\dfrac{2\sqrt{at} + z}{2\sqrt{t}}],\ A_{16} = erf[\dfrac{2\sqrt{at} - z}{2\sqrt{t}}],\ A_{17} = erf[\dfrac{2\sqrt{at} + z}{2\sqrt{t}}],\ A_{18} = e^{-2z\sqrt{\frac{aP_r}{-1+P_r}}},$

$A_{19} = e^{-2z\sqrt{\frac{aS_c}{-1+S_c}}}.\ A_{20} = erf[\dfrac{z - 2t\sqrt{\frac{aP_r}{-1+P_r}}}{2t}]\ A_{21} = erf[\dfrac{z + 2t\sqrt{\frac{aP_r}{-1+P_r}}}{2t}],\ A_{22} = erf[\dfrac{2t\sqrt{\frac{a}{-1+P_r}} - z\sqrt{P_r}}{2t}],$

$A_{23} = erf[\dfrac{2t\sqrt{\frac{a}{-1+P_r}} - z\sqrt{P_r}}{2t}],\ A_{24} = erf[\dfrac{2t\sqrt{\frac{a}{-1+P_r}} + z\sqrt{P_r}}{2t}],\ A_{25} = erf[\dfrac{z - 2t\sqrt{\frac{aS_c}{-1+S_c}}}{2t}],$

$A_{26} = erf[\dfrac{z + 2t\sqrt{\frac{aS_c}{-1+S_c}}}{2t}],\ A_{27} = erf[\dfrac{2t\sqrt{\frac{a}{-1+S_c}} - 2\sqrt{S_c}}{2t}],\ A_{28} = erf[\dfrac{2t\sqrt{\frac{a}{-1+S_c}} + 2\sqrt{S_c}}{2t}].$

Biographical notes

Dr Uday Singh Rajput is a faculty member in the department of mathematics and astronomy, University of Lucknow, India. He has more than 25 years of teaching experience at UG and PG levels and also guided students for Ph D degree. He has published more than 70 research articles. His research areas include MHD flows, Graph Theory and Operations Research.

Gaurav Kumar is a research student in the department of mathematics and astronomy, University of Lucknow, India.